

Article

# Nucleation and Initial Growth of Garnet in Low-Grade Metamorphic Rocks of the Sanbagawa Metamorphic Belt, Kanto Mountains, Japan

Mutsuko Inui \* , Yumenosuke Wakai and Hiirou Sakuragi

School of Science and Engineering, Kokushikan University, 4-28-1 Setagaya, Setagaya-ku, Tokyo 154-8515, Japan

\* Correspondence: inui@kokushikan.ac.jp

Received: 23 February 2020; Accepted: 22 March 2020; Published: 24 March 2020



**Abstract:** The beginning of the recrystallization of minerals within a subducting oceanic plate provides a valuable record of dehydration within the subduction zone. Pelitic schists of the Nagatoro area, Kanto Mountains, Japan, record the initial stages of garnet growth. Consequently, these rocks were studied to analyze garnet nucleation and growth during metamorphism of the Sanbagawa metamorphic belt, one of the world's most comprehensively studied subduction complexes. The garnet grains are small, euhedral, and occur only within micaceous lamellae that define the schistosity. Crystal size distribution analyses revealed most of the garnet grains follow the log-normal size distribution, indicating that they formed in the same event. A few exceptionally large garnet grains exist that do not seem to follow the log-normal distribution. The latter garnet grains contain a rounded fragmental area with a different chemical composition inside the core. It is possible that detrital fragments of garnet contribute to the irregular crystal size distribution of garnet in the studied area. Many of the smaller (log-normal) garnet grains have relatively large, homogeneous Mn-rich cores. The lack of chemical zoning within the garnet cores suggests that they grew under constant pressure and temperature in response to overstepping of the garnet-in reaction. The chemical composition changes very sharply at the boundary between the core and the surrounding mantle. The size of the Mn-rich core is different from sample to sample, suggesting that the nucleation was controlled by the local chemical condition of each sample.

**Keywords:** garnet; chemical zoning; crystal size distribution; nucleation; overstepping

## 1. Introduction

The beginning of recrystallization within a subducting oceanic plate is of particular interest because it records the initiation of dehydration within the subduction zone. Garnet-forming reactions are one of the most common types of dehydration reactions that affect subducting crustal rocks [1]. Garnet is widespread in metamorphic rocks because it is stable over a wide range of pressures and temperatures for the bulk compositions most commonly found in sedimentary rocks [2]. The contact between garnet-bearing and garnet-free rocks is often plotted on geological maps as an isograd and used as an indication of metamorphic grade. Garnet is useful to petrologists because compositional growth zoning can be used to quantify metamorphic conditions under the assumption of chemical equilibrium [3,4]. Zoning profiles have also been used as an indicator of the history of garnet growth and metamorphism [5–7]. The extensive use of garnet in thermobarometric studies has motivated investigations of its crystallization process in addition to its thermodynamic properties, such as controls by bulk rock chemistry [8], controls by fluids [9], the extent of equilibrium during growth [10,11], and crystal size distribution [12]. Garnet grows during continuous reactions that are controlled by pressure, temperature, and other thermodynamic parameters. It is thought that thermal

overstepping is required to initiate nucleation. Spear et al. explored the magnitude and consequences of overstepping [13], and Gaidies et al. investigated the role of interfacial energy using forward models of garnet formation [14]. These studies were based on analyses of large well-grown garnet grains or theoretical calculations; there are few descriptions of the initiation of garnet nucleation and growth in natural samples.

Low-grade pelitic schists of the Sanbagawa metamorphic belt are exposed in the Nagatoro area of the Kanto Mountains, Japan, and these rocks provide an ideal opportunity to study the initiation of recrystallization to form metamorphic garnet. The Sanbagawa metamorphic belt is a high-pressure-temperature ( $P$ - $T$ ) metamorphic belt that crops out in central to southwestern Japan. It is one of the most intensively studied subduction-related metamorphic belts worldwide [15]. Garnet occurs in patches within the Nagatoro area, which is mapped as part of the chlorite zone and is nominally garnet-free. Observations of these garnets provide insights into the initiation of garnet recrystallization in subducting sedimentary rocks. In this study, small garnet grains within low-grade pelitic schists were analyzed to obtain the crystal size distribution and determine their internal chemical zoning. The results indicate that the growth history of the larger and smaller garnet should be discussed separately in the study area. The larger garnet was investigated to show the contribution of detrital fragments. The nucleation and growth of the smaller grains were analyzed to show that the beginning of garnet recrystallization presumably required overstepping conditions and was controlled by the local chemistry in the rock.

## 2. Geological Setting

The Sanbagawa metamorphic belt, located on the eastern margin of the Asian continent [15], was once part of an accretionary complex and consists mainly of metapelites, metabasalts, and metacherts. Isotopic evidence suggests that accretion of the protolith and metamorphism occurred during the Late Cretaceous [16], although the timing of these events differs between the eastern and western parts of the belt. The highest-grade rocks, which are exposed in central Shikoku, were metamorphosed to the eclogite facies at  $\sim 700$  °C and  $\sim 1.5$  GPa [7,17]. Higashino identified metamorphic zones within the lower-grade rocks of central Shikoku, based on the mineral assemblages of pelitic schists [18]. In order of ascending grade, these are the chlorite, garnet, albite-biotite, and oligoclase-biotite zones. The peak  $P$ - $T$  conditions estimated for the garnet zone is 440 °C and 0.6 GPa [17] and characteristic of greenschist facies conditions. It is likely that the garnet formation records the first major dehydration and recrystallization event during the subduction of these rocks.

The Nagatoro area is located to the northwest of Tokyo, within the Kanto Mountains, and forms the easternmost part of the Sanbagawa metamorphic belt. The Kanto Mountains can be divided roughly into chlorite, garnet, and biotite zones, with increasing metamorphic grade, based on the mineral assemblages and extent of graphitization in pelitic schists [19,20]. The bedding in this area is sub-parallel to the schistosity [19,20]. Pelitic schists of the chlorite zone generally contain quartz, plagioclase, muscovite, and chlorite, with accessory calcite, titanite, and pyrite. Schists of the garnet zone contain the same assemblage, with the addition of garnet. Schists of the chlorite zone are common in the Nagatoro area, with localized occurrences of garnet- and biotite-zone schists [20].

The samples investigated in this study are from an outcrop that contains localized garnet-bearing patches, as described [21] (Figure 1). These authors plotted the distribution of garnet-bearing rocks within the outcrop and inferred that the localized garnet distribution was not caused by structural juxtaposition and that the peak metamorphic  $P$  and  $T$  were close to garnet-in conditions. Inui et al. estimated peak metamorphic temperatures for this outcrop of  $\sim 400$ – $450$  °C using a geothermometer based on the Raman spectra of carbonaceous material [22]. This temperature is consistent with the estimated peak temperature of equivalent garnet zone rocks in central Shikoku ( $440 \pm 15$  °C; [17]).

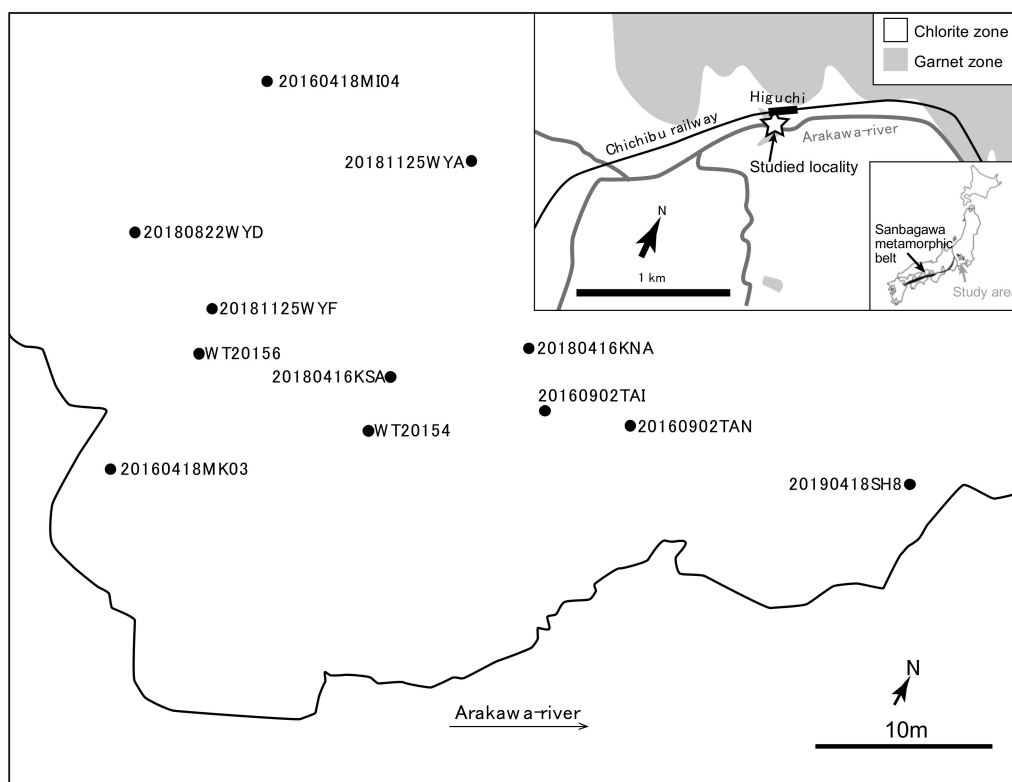


**Figure 1.** Locality map of this study. Modified after Hashimoto et al. [20]. Chlorite zone is the Zone I in [20] which is the lowest grade zone. Garnet appears in the Garnet zone (Zone II in [20]).

### 3. Materials and Methods

The garnet-bearing pelitic schists were sampled (Figure 1), and the mineral assemblages, textures, and garnet distribution were observed using a polarizing microscope. The garnet crystal size distribution was measured using backscattered electron images (BEIs) obtained on a JEOL JSM-6010LA (JEOL, Tokyo, Japan) scanning electron microscope (SEM) at Kokushikan University, Tokyo, Japan. The data derived from the two-dimensional (2D) surface of the thin sections were converted into a three-dimensional (3D) size distribution dataset using the computational correction method of Peterson [23]. The size of the core part observed in the BEIs was measured. Mapping and semi-quantitative point analyses of garnet composition were performed using energy-dispersive X-ray spectroscopy (EDS) on the SEM described above, using an acceleration voltage of 20.0 kV and 15.0 kV. The point analyses are semi-quantitative because the instrument cannot be calibrated using standard samples. Abbreviations of the names of minerals and end-member components are from Whitney and Evans [24].

### 4. Results

#### 4.1. Outcrop Description, Mineral Assemblages, and Textures

Pelitic schists and minor mafic schists are the most common rock types at the sampling locality. The color of the pelitic schists varies from lighter psammites to darker pelites. All non-mafic schists are referred to as pelitic here. The most common assemblage is quartz + muscovite + albite + chlorite + titanite ± garnet ± calcite ± epidote ± carbonaceous material. The schistosity is defined by micaceous lamellae, ~1.0 mm thick. Relatively siliceous assemblages occur in the intervals between the micaceous lamellae. Chlorite, albite, titanite, and garnet are commonly associated with muscovite (Figure 2).

Garnet is exclusively located within the micaceous lamellae, where it is surrounded by muscovite and sometimes chlorite. The garnet grains are small and euhedral, with diameters mostly <100 μm, and are distributed heterogeneously within the mica-rich lamellae. Not all micaceous lamellae within

a thin section contain garnet and some parts of garnet-bearing lamellae are garnet-free, such that garnet is concentrated locally within the lamellae. This garnet distribution is generally consistent with previous descriptions of the same outcrop [21].

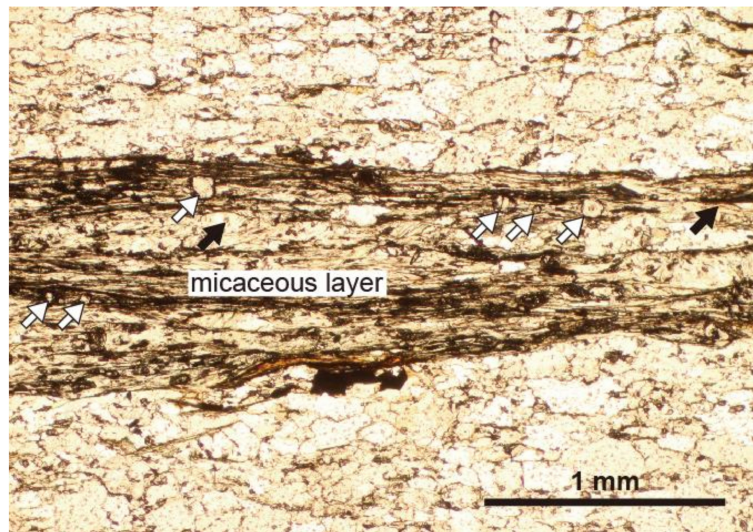


**Figure 2.** Photomicrograph of a polarizing microscope (plane-polarized light). Sample No. 20181125WYF. Micaceous lamella that defines the schistosity is seen in the center of the photo. Muscovite, chlorite, albite, and titanite are common in the micaceous lamellae. Carbonaceous material is often contained in albite and muscovite (black arrows). Upper and lower areas are mainly quartz. Euhedral garnet grains (white arrows) are exclusively found in the micaceous lamella.

#### 4.2. Crystal Size Distribution of Garnet

The sizes of garnet grains in four thin sections were measured to determine their crystal size distributions. The measurements were performed using BEIs, so the data were taken from a 2D slice of each sample. The diameter of elongate grains was taken to be that of the longest direction. Grain sizes were measured within an area of  $\sim 1 \text{ cm}^2$  on each thin section. This area was not measured precisely because the absolute number density depended strongly on whether the investigated area contained concentrations of garnet, so the absolute number of garnets was highly variable and was considered immaterial for the purpose of this study. The distribution of 2D grain diameter based on 30 to 100+ garnet grains in each thin section, is shown in Figure 3. The mode of garnet size for all four samples is between 30 and 50  $\mu\text{m}$ . A small number of larger grains with diameters of  $>100 \mu\text{m}$  are present in three of the four samples.

In order to estimate whether or not the larger grains are exceptional, the crystal size distribution histogram was studied. The 2D grain diameters were computationally converted into a 3D dataset using the method of Peterson [21] (Figure 4). The vertical axis in Figure 4 is dimensionless because the aim is to show the shape of the histogram, rather than the absolute number density of garnet grains. The result shows that the 3D crystal size distribution is approximately log-normal for grains up to  $\sim 80 \mu\text{m}$  in diameter. It is interpreted that crystals of  $>100 \mu\text{m}$  in diameter are exceptionally large, based on an extrapolation of the log-normal curve defined by the smaller grains. Hereafter, the smaller grains with a log-normal size distribution, which are the majority, are called the smaller garnet (grains). The exceptionally large grains are called the larger garnet (grains). The larger grains are found in samples WT20156 and 20181125WYF. The largest of the grains in WT20154 is also  $>100 \mu\text{m}$  in diameter though it is not clear from the shape of the histogram if they are the larger garnet.

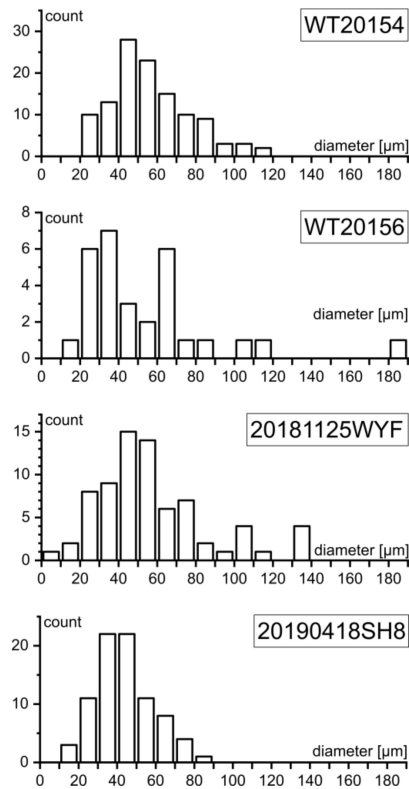


**Figure 3.** Crystal size distribution measured in 2D of garnet in 4 thin sections. Diameter was measured using backscattered electron images. Some of the largest grains seem exceptionally large.

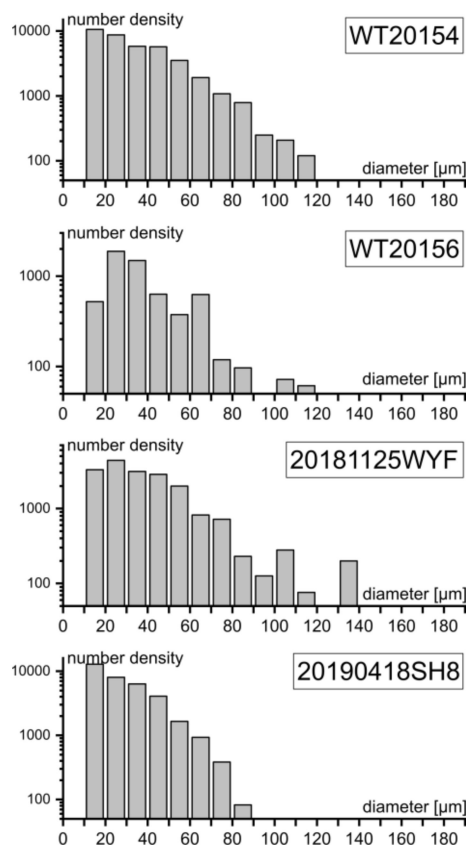


**Figure 4.** 2D crystal size distribution in Figure 3 converted into 3D number density. Samples No. WT20156 and No. 20181125WYF contain the larger garnet grains that exist more frequently than expected.

### 4.3. Garnet Compositions

Backscattered electron images (BEIs) of the smaller and larger garnet grains on the four thin sections were investigated (Figure 5). The chemical profile of the same grains from the core to the rim obtained by semi-quantitative analyses using the EDS is also shown in Figure 5. Thirty to 100+ grains had BEIs taken for each sample. The smaller garnet commonly shows a light contrast core near the grain center (Figure 5a,b). The shape of the core is euhedral to subhedral. The light contrast represents a material with a relatively high atomic number and corresponds in this case to areas enriched in spessartine (Mn end-member) as shown in the associated compositional profile (Figure 5c,d). The Mn-rich cores in the smaller garnet grains are relatively homogeneous, which is also illustrated in the chemical mapping images (Figure 6). Very small irregularly shaped areas, poor in spessartine, were observed in some grains (Figure 6c). The chemical boundary between the core and the surrounding mantle is very sharp on the BEIs. The sharpness indicates that the chemical zoning is related to grain growth, not being altered by later chemical diffusion. BEIs of the larger garnet grains in the same sample also exhibits an Mn-rich area inside the grains, though their shape is more complex (Figure 5e,f). An irregularly shaped Mn-poor area is found inside the Mn-rich core (Figure 6e–h). The Mn-rich core seems to have overgrown on the area. Spessartine decreases and grossular (Ca end-member) increases sharply at the outline of the Mn-rich core, regardless of the grain size. The mantles of all grains are enriched in grossular. Spessartine and grossular gradually decrease toward the rim.

The results of semi-quantitative point analyses are shown in the table and the triangular diagram (Table 1 and Figure 7). Though the data are not quantitatively accurate, it is demonstrated that the different grains show similar chemical trends except the rounded fragmental part inside the Mn-rich cores of the larger grains. Approximative estimates are, the Mn-rich cores of the smaller and larger grains have spessartine mole fractions of ~60% (~27 wt % Mn), and the grossular mole fraction of the Ca-rich mantles is ~35% (~16 wt % Ca). It is consistent that the grains grew under conditions not far from equilibrium, except for the Fe-rich fragments inside the Mn-rich core. Relatively high spessartine mole fraction (>30%) at the rim indicates that the growth ceased at low metamorphic conditions.

**Table 1.** Representative chemical composition of garnet analyzed semi-quantitatively by energy-dispersive X-ray spectroscopy (EDS). Automatically normalized to make the total 100%.

Grain Number (wt %)	Grain 65			Grain 01	
	Mn-Rich Core	Mantle	Fragment Inside Core	Mn-Rich Core	Mantle
SiO <sub>2</sub>	41.57	41.61	41.63	41.64	41.87
TiO <sub>2</sub>	0.16	0.14	0.12	0.18	0.10
Al <sub>2</sub> O <sub>3</sub>	13.81	13.76	13.56	13.72	13.72
FeO *	9.71	12.21	19.11	9.36	12.75
MnO	26.58	16.08	12.77	27.34	15.03
MgO	0.20	0.26	2.40	0.25	0.35
CaO	7.90	15.84	10.31	7.42	16.11
Total	100.00	100.00	100.00	100.00	100.00

\* Total iron as FeO.

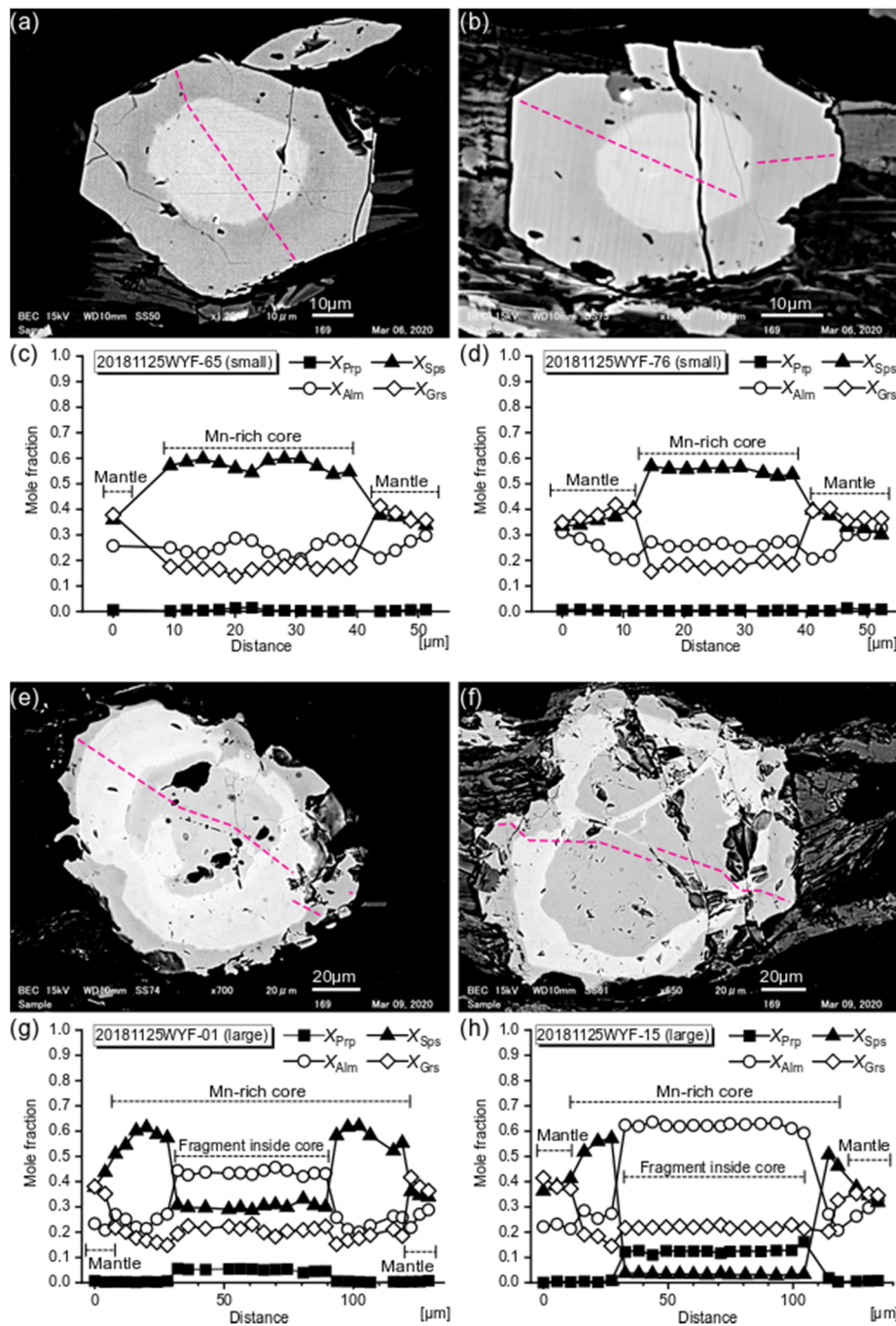


**Figure 5.** Backscattered electron images (BEIs) of garnet grains in one thin section together with the compositional profile obtained by semi-quantitative energy-dispersive X-ray spectroscopy (EDS) analyses. Pink dotted lines on BEIs show where line analyses were performed. Sample no. 20181125WYF. (a) and (b): BEIs of grains No. 65 and No. 76, respectively, which are presumably the smaller garnet grains that show log-normal crystal size distribution. (c) and (d): compositional profile of grains shown in (a) and (b). (e) and (f): BEIs of grains No.01 and No.15, respectively, which are exceptionally large concerning the log-normal crystal size distribution (see text). (g) and (h): compositional profile of grains shown in (e) and (f).

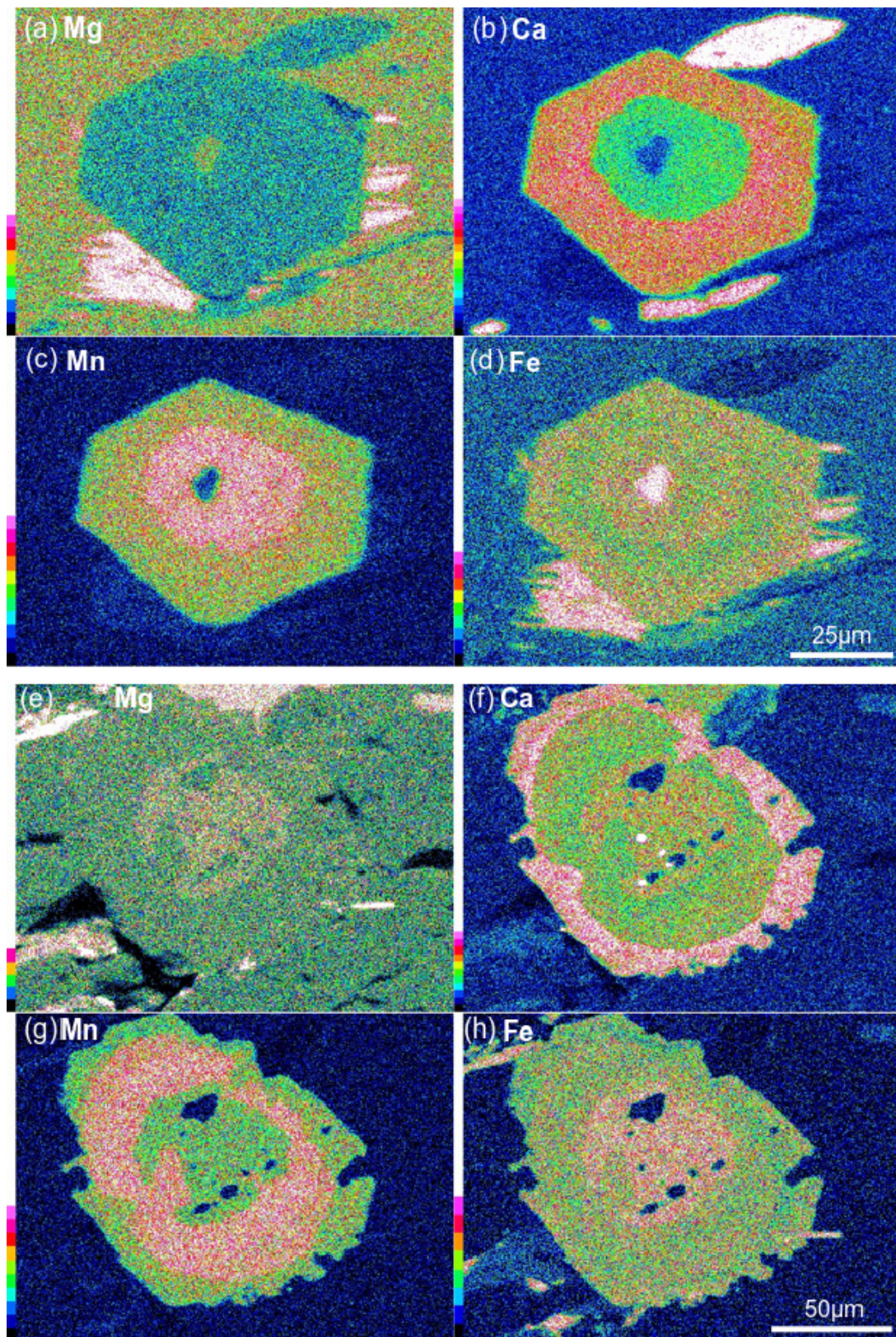


**Figure 6.** Chemical mapping image of garnet in sample no. 20181125WYF. (a–d): Mapped profile of Mg, Ca, Mn, and Fe, respectively, of grain no.65 (Figure 5a,c). An example of the smaller log-normal garnet. (e–h): Mapped profile of Mg, Ca, Mn, and Fe, respectively, of grain no.1 (Figure 5e,g). One of the larger garnet grains.

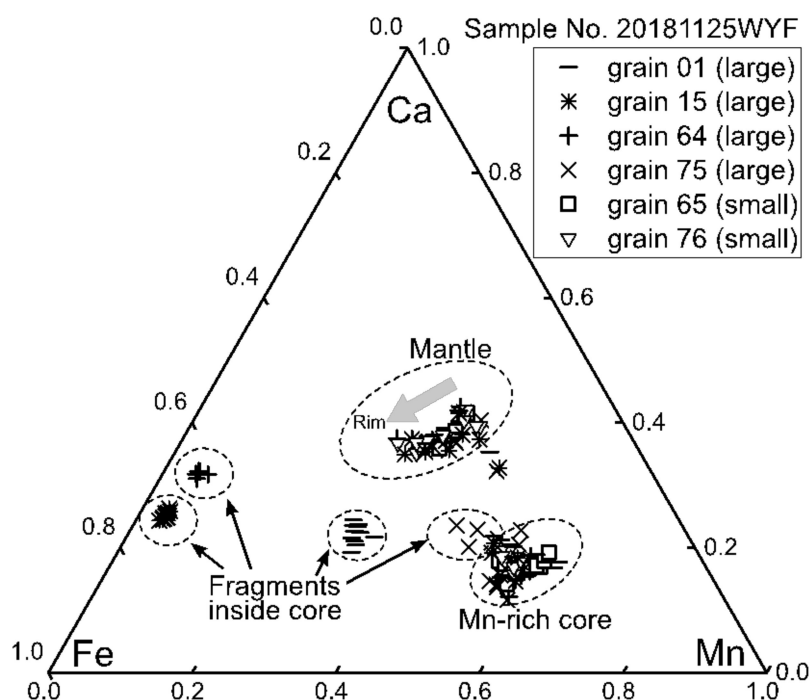


**Figure 7.** Triangular plot of the chemical trend of garnet grains from the core to the rim obtained from semi-quantitative analyses by EDS. All grains are from sample 20181125WYF. The chemical composition of the Mn-rich cores and the Ca-rich mantles are similar in all grains, whereas that of the Fe-rich fragments inside the Mn-rich cores in larger grains vary from grain to grain.

#### 4.4. Sizes of Manganese-Rich Cores

The Mn-rich cores occur differently from sample to sample. Larger garnet grains contained the Mn-poor, Fe-rich part inside the Mn-rich core as described above. The cores of the smaller garnet grains are homogeneously rich in Mn, however, the occurrence and the size of the Mn-rich core are dependent on samples. Garnet grains in some samples frequently show the Mn-rich core, but those in other samples do not. The size of the Mn-rich core in relation to that of the grain seems to be different from sample to sample. Figure 8 shows the diameters of the cores plotted along with the grain diameters derived from the BEI images for eight samples that only contain garnet grains smaller than 90  $\mu\text{m}$ .

For example, the garnet in sample 20180416KSA has smaller cores than in other samples, whereas the grain diameters are larger than in other samples. These observations indicate that garnet growth was thermodynamically controlled on the thin section scale, but not on the outcrop scale and that the conditions of garnet nucleation and growth varied among the samples. Artifacts might have been introduced by the 2D, rather than 3D, measurements. In particular, the seemingly coreless grains may have cores that are not observable due to cutting effects. However, the results are sufficiently robust to justify further discussion.

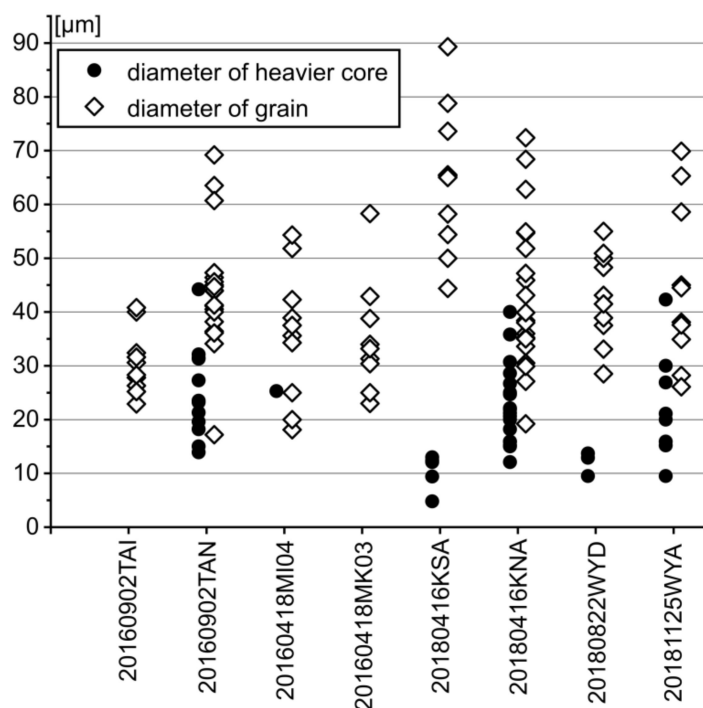


**Figure 8.** Diameter of garnet grain and Mn-rich core. The number of plots for the diameters of Mn-rich cores is fewer since it is not plotted when the Mn-rich core is not observable on the BEI. The size of the Mn-rich cores is relatively small in samples 20180416KSA and 20180822WYD. Mn-rich cores are not observed in samples 20160902TAI and 20160418MK03.

## 5. Discussion

### 5.1. Insight into Metamorphic Nucleation of Garnet

Crystal size distribution analyses of garnet performed in this study suggested that the majority of the garnet grains were formed by the same event since they showed log-normal size distribution. However, the existence of the larger garnet grains, approximately 100  $\mu\text{m}$  or more in diameter, was difficult to explain. The results of the chemical analyses revealed that the Mn-rich cores of the larger grains contain Fe-rich fragmental parts inside them. The shape of the fragments is irregular, whereas those of the surrounding Mn-rich cores are subhedral. It is comprehensible if the larger garnet grains observed in this study are exceptionally large because they started growing onto some exceptionally large fragment of existent garnet. The chemical composition of the fragments is generally much poorer in Mn and richer in Fe and Mg compared to the other parts of the garnet. The chemical composition cannot be attributed to the low-grade metamorphic conditions of the Nagatoro area. Considering the fact that the chemical composition of the fragments varies from grain to grain, it is reasonable to interpret that the fragments have a detrital origin. It is possible that detrital garnet existed in the sedimentary rocks without any involvement in metamorphic reactions during the low-grade stage. The detrital garnet was surrounded by metamorphic overgrowth when the condition reached the garnet stability field so that the detrital fragments were kept out of the metamorphic equilibrium. The two samples that contained larger grains, W20156 and 20181125WYF, were found close to each other in the outcrop (Figure 1). It is possible that the detrital garnet occurs very locally.

The fact that the Mn-rich core of the smaller garnet is chemically homogeneous indicates that the whole core part grew under constant  $P$ - $T$  conditions. The smaller garnet grains recognized in this study seem to be the ones examined by a previous study [21], based on their size and the chemical zoning profile. It is suggested in this study that the grains with the diameter approximately 80  $\mu\text{m}$  or less were formed by the same nucleation event judged by their log-normal crystal size distribution. Their Mn-rich core is chemically homogeneous and euhedral to subhedral. The diameter of the Mn-rich

core is generally around half the diameter of the grain, which is relatively large. If garnet started to form precisely at the theoretical nucleation temperature, it is expected it would be infinitesimally small and would not grow larger unless the temperature increased. When the temperature increased, the Mn content in the new garnet should decrease because of the change in chemical equilibrium between chlorite, and also because the bulk rock (namely chlorite) chemistry would be more depleted in Mn [25]. It is impossible to produce a homogeneous core through gradual growth during a temperature increase without later alteration by diffusion. The clear outline of the Mn-rich core observed in the BEIs indicates that the chemical zoning was not altered after growth. Thus, the homogeneous Mn-rich core observed in this study must have formed at once in a certain  $P$ - $T$  condition. To produce new garnet crystals in such observable volume, it is reasonable to assume a certain degree of overstepping of  $P$ - $T$  conditions [26]. It is possible that those subhedral Mn-rich cores with the diameter approximately 10  $\mu\text{m}$  to 30  $\mu\text{m}$  are the first recrystallized garnet nuclei formed by the metamorphism.

Heterogeneous distribution of garnet nucleation within the thin section indicates the heterogeneous chemical potential of elements within rocks. Garnet exclusively occurs within the micaceous lamellae. Garnet sometimes concentrates in certain lamella but does not occur in others. The size of the Mn-rich core also differs from sample to sample. It is likely that the alternating micaceous and quartzose lamellae supplied different chemical conditions. The fugacity of the fluid phase was expected to be low during the early stage of garnet recrystallization since one of the major water-forming (dehydration) reaction in the subducted sedimentary rocks was the formation of garnet itself. Lacking the intergranular fluid, relatively sluggish material transport is expected within the rock. It seems likely that the garnet grains nucleated controlled by the rate of material transport. As a result, garnet nucleated and grew where they had abundant reactants, namely in the micaceous layer, as argued by the previous study [11].

The very small irregularly shaped Mn-poor area observed at the center of some of the smaller garnet has also been interpreted as detrital garnet [21]. Observation in this study is consistent with the interpretation. Though the Mn-poor area is too small to make accurate quantitative analyses, the chemical mapping image of the area shows Mn-poor and Fe- and Ca-rich trend, which is equivalent to the previous report. Observation in this study discovered more of that small Mn-poor area, revealing that it is common to contain such a small Mn-poor area at the center of the newly recrystallized garnet. It is not clear whether this is equivalent to the large rounded fragment discussed above. Though the size and shape are considerably different, no large difference is recognized concerning the chemical composition trend on the mapping images. The role of the existent garnet on the nucleation process is yet to be investigated.

### 5.2. Growth Process of Garnet and Geologic Implication

The growth of garnet after the formation of the Mn-rich core, either overgrown or nucleated, shows a similar chemical trend in different grains in this study; formation of the Mn-poor, Ca-rich mantle. It is consistent to assume that the growth occurred simultaneously. However, it is indicated from the heterogeneous garnet occurrence, and also from the different sizes of the initial Mn-rich core, that the chemical condition was heterogeneous within the rock as discussed in the previous section. The previous study reports garnet grains with different chemical zoning from a nearby outcrop [21]. It is possible that the garnet chemical composition is slightly different from sample to sample, controlled by the bulk rock condition in the thin section scale. A sharp change of chemical composition is recognized in the BEIs between the Mn-rich core and the Ca-rich mantle, both in the smaller and larger garnet. The sharp boundary, however, does not necessarily require a sharp change of the metamorphic condition during the growth of the garnet. After the formation of the Mn-rich core, the driving force of the garnet formation must have decreased since the overstepping was dissolved. Mn was depleted from the bulk rock environment. It is reasonable to assume that the growth restarted when the Ca content of garnet became more stable. Faryad and Ježek calculated garnet growth considering bulk fractionation and predicted a jump in garnet formation condition, which results in a sharp change of chemical composition after forming a homogeneous core, just as observed in this study [27].

In conclusion, it is interpreted that the local occurrence of garnet grains in the Nagatoro area records the beginning of garnet recrystallization controlled by the local chemistry in the thin section scale. Many of the garnet grains preserved clearly outlined homogeneous Mn-rich cores with similar size, which indicates growth under overstepping condition. The log-normal crystal size distribution was consistent with their simultaneous growth. Relatively high spessartine content at the garnet rim suggests that the metamorphic condition was still low when garnet growth ceased. It is indicated that the rock was quenched not long after reaching the garnet stability field. Some of the larger garnet grains were exceptionally large in light of the crystal size distribution. In those grains, the Mn-rich cores contained garnet fragments inside, which presumably have a detrital origin. The garnet size distribution in the early stage is possibly dependent on the existence of the detrital garnet.

## 6. Conclusions

Crystal size distribution and chemical zoning of garnet grains in the pelitic schists of the Nagatoro area were investigated to discuss the beginning of the recrystallization in the Sanbagawa metamorphic belt. The garnet grains are small, euhedral, and occur only within micaceous lamellae indicating that the nucleation occurred controlled by the local chemical condition. Crystal size distribution analyses revealed that not all the garnet grains follow the log-normal size distribution, but a few exceptionally large grains exist. The larger garnet grains contain rounded fragmental area inside the core. The chemical composition of the fragmental area was different from grain to grain, suggesting the contribution of detrital garnet to their irregularly large crystal size. It is reasonable to assume that the smaller garnet grains, which are the majority, formed in the same event during metamorphism since they show log-normal size distribution. The homogeneous Mn-rich cores suggest that they grew under constant pressure and temperature in response to overstepping of the condition. The different size of the Mn-rich core from sample to sample indicates that the formation of the core was controlled by the local chemical condition of each sample. The beginning of garnet recrystallization presumably required an overstepping condition to form the core, controlled by the local chemistry of the rock.

**Author Contributions:** Conceptualization, M.I.; Methodology, M.I.; Validation, M.I.; Investigation, Y.W., H.S., and M.I.; Resources, Y.W., H.S., and M.I.; Data curation, Y.W., H.S., and M.I.; Writing—original draft preparation, M.I.; Writing—review and editing, M.I.; Visualization, Y.W., H.S., and M.I.; Supervision, M.I.; Project administration, M.I. All authors have read and agreed to the published version of the manuscript.

**Funding:** This research received no external funding.

**Acknowledgments:** We are grateful to the two reviewers, for their comments encouraged us a lot to make additional analyses and improve our presentation. We thank T. Watanabe for discovering the queer zoning in garnet which inspired the research. We thank M. Inoue for the information and arrangement for our sampling survey, R. Ogawa and T. Sakurai for their arrangement and attendance to our survey. We thank M. Uno for providing aerial photographs of the outcrop which is very useful for our sampling. We gratefully acknowledge colleagues of the laboratory at the Kokushikan University, especially those who supplied and organized their samples for use in this study.

**Conflicts of Interest:** The authors declare no conflict of interest.

## References

1. Dragovic, B.; Samanta, L.M.; Baxter, E.F.; Selverstone, J. Using garnet to constrain the duration and rate of water-releasing metamorphic reactions during subduction: An example from Sifnos, Greece. *Chem. Geol.* **2012**, *314*, 9–22. [[CrossRef](#)]
2. Symmes, G.H.; Ferry, J.M. The effect of whole-rock MnO content on the stability of garnet in pelitic schists during metamorphism. *J. Metamorph. Geol.* **1992**, *10*, 221–237. [[CrossRef](#)]
3. Tracy, R.J.; Robinson, P.; Thompson, A.B. Garnet composition and zoning in the determination of temperature and pressure of metamorphism, central Massachusetts. *Am. Mineral.* **1976**, *61*, 762–775.
4. Holdaway, M.J. Application of new experimental and garnet Margules data to the garnet-biotite geothermometer. *Am. Mineral.* **2000**, *85*, 881–892. [[CrossRef](#)]

5. Spear, F.S.; Selverstone, J. Quantitative P-T paths from zoned minerals: Theory and tectonic applications. *Contrib. Mineral. Petrol.* **1983**, *83*, 348–357. [[CrossRef](#)]
6. Sakai, C.; Banno, S.; Toriumi, M.; Higashino, T. Growth history of garnet in pelitic schists of the Sanbagawa metamorphic terrain in central Shikoku. *Lithos* **1985**, *18*, 81–95. [[CrossRef](#)]
7. Aoya, M.P.-T.-D. Path of Eclogite from the Sambagawa Belt Deduced from Combination of Petrological and Microstructural Analyses. *J. Petrol.* **2001**, *42*, 1225–1248. [[CrossRef](#)]
8. Pattison, D.R.M.; Seitz, J.D. Stabilization of garnet in metamorphosed altered turbidites near the St. Eugene lead-zinc deposit, southeastern British Columbia: Equilibrium and kinetic controls. *Lithos* **2012**, *134*, 221–235. [[CrossRef](#)]
9. Skelton, A.D.L. The effect of metamorphic fluid flow on the nucleation and growth of garnets from Troms, North Norway. *J. Metamorph. Geol.* **1997**, *15*, 85–92. [[CrossRef](#)]
10. Chernoff, C.B.; Carlson, W.D. Disequilibrium for Ca during growth of pelitic garnet. *J. Metamorph. Geol.* **1997**, *15*, 421–438. [[CrossRef](#)]
11. Spear, F.; Daniel, C. Diffusion control of garnet growth, Harpswell Neck, Maine, USA. *J. Metamorph. Geol.* **2001**, *19*, 179–195. [[CrossRef](#)]
12. Marsh, B.D. Crystal size distribution (CSD) in rocks and the kinetics and dynamics of crystallization I. Theory. *Contrib. Mineral. Petrol.* **1988**, *99*, 277–291. [[CrossRef](#)]
13. Spear, F.; Thomas, J.; Hallett, B. Overstepping the garnet isograd: A comparison of QuiG barometry and thermodynamic modeling. *Contrib. Mineral. Petrol.* **2014**, *168*, 1059–1073. [[CrossRef](#)]
14. Gaidies, F.; Pattison, D.R.M.; de Capitani, C. Toward a quantitative model of metamorphic nucleation and growth. *Contrib. Mineral. Petrol.* **2011**, *162*, 975–993. [[CrossRef](#)]
15. Banno, S.; Sakai, C. Geology and metamorphic evolution of the Sanbagawa belt. In *Evolution of Metamorphic Belts*; Daly, J.S., Cliff, R.A., Yardley, B.W.D., Eds.; Geological Society: London, UK, 1989; Volume 43, pp. 519–532.
16. Tsutsumi, Y.; Miyashita, A.; Terada, K.; Hidaka, H. SHRIMP U-Pb dating of detrital zircons from the Sanbagawa Belt, Kanto Mountains, Japan: Need to revise the framework of the belt. *J. Mineral. Petrol. Sci.* **2009**, *104*, 12–24. [[CrossRef](#)]
17. Enami, M.; Wallis, S.R.; Banno, Y. Paragenesis of sodic pyroxene-bearing quartz schists: Implications for the P-T history of the Sanbagawa belt. *Contrib. Mineral. Petrol.* **1994**, *116*, 182–198. [[CrossRef](#)]
18. Higashino, T. The higher grade metamorphic zonation of the Sambagawa metamorphic belt in central Shikoku, Japan. *J. Metamorph. Geol.* **1990**, *8*, 413–423. [[CrossRef](#)]
19. Sakai, C. Biotite zone in the Sambagawa metamorphic terrain east of Onishi-machi, Kanto Mountains. *J. Geol. Soc. Jpn.* **1980**, *86*, 517–524, (In Japanese with English abstract). [[CrossRef](#)]
20. Hashimoto, M.; Tagiri, M.; Kusakabe, K.; Masuda, K.; Yano, T. Geologic structure formed by tectonic stacking of sliced layers in the Sanbagawa metamorphic terrain, Kodama-Nagatoro area, Kanto Mountains. *J. Geol. Soc. Jpn.* **1992**, *98*, 953–965, (In Japanese with English abstract). [[CrossRef](#)]
21. Inui, M.; Tanifuji, A. Spatial distribution of garnet indicating control of bulk rock chemistry in the Sanbagawa metamorphic rocks, Kanto Mountains, Japan. *J. Mineral. Petrol. Sci.* **2018**, *113*, 181–189. [[CrossRef](#)]
22. Inui, M.; Izumi, R.; Watanabe, T. Estimated peak metamorphic temperature of the Sanbagawa schists from Nagatoro area, Kanto Mountains, using Raman microspectrometry on carbonaceous materials. *Trans. Kokushikan Univ. Fac. Sci. Eng.* **2017**, *11*, 55–60.
23. Peterson, T.D. A refined technique for measuring crystal size distributions in thin section. *Contrib. Mineral. Petrol.* **1996**, *124*, 395–405. [[CrossRef](#)]
24. Whitney, D.L.; Evans, B.W. Abbreviations for names of rock-forming minerals. *Am. Mineral.* **2010**, *95*, 185–187. [[CrossRef](#)]
25. Inui, M.; Toriumi, M. A theoretical study on the formation of growth zoning in garnet consuming chlorite. *J. Petrol.* **2004**, *45*, 1369–1392. [[CrossRef](#)]
26. Wolfe, O.M.; Spear, F.S. Determining the amount of overstepping required to nucleate garnet during Barrovian regional metamorphism, Connecticut Valley Synclinorium. *J. Metamorph. Geol.* **2018**, *36*, 79–94. [[CrossRef](#)]
27. Faryad, S.W.; Ježek, J. Compositional zoning in garnet and its modification by diffusion during pressure and temperature changes in metamorphic rocks; an approach and software. *Lithos* **2019**, *332*, 287–295. [[CrossRef](#)]

